Pulse repetition rate scaling from 5 to 100 GHz with a high-power semiconductor disk laser

Mario Mangold, Christian A. Zaugg, Sandro M. Link, Matthias Golling, Bauke W. Tilma, and Ursula Keller

Department of Physics, Institute for Quantum Electronics, ETH Zürich, 8093 Zürich, Switzerland
*mangoldm@phys.ethz.ch

Abstract: The high-power semiconductor laser studied here is a modelocked integrated external-cavity surface emitting laser (MIXSEL), which combines the gain of vertical-external-cavity surface-emitting lasers (VECSELs) with the saturable absorber of a semiconductor saturable absorber mirror (SESAM) in a single semiconductor layer stack. The MIXSEL concept allows for stable and self-starting fundamental passive modelocking in a simple straight cavity and the average power scaling is based on the semiconductor disk laser concept. Previously record-high average output power from an optically pumped MIXSEL was demonstrated, however the long pulse duration of 17 ps prevented higher pulse repetition rates and many interesting applications such as supercontinuum generation and broadband frequency comb generation. With a novel MIXSEL structure, the first femtosecond operation was then demonstrated just recently. Here we show that such a MIXSEL can also support pulse repetition rate scaling from ≈5 GHz to >100 GHz with excellent beam quality and high average output power, by mechanically changing the cavity length of the linear straight cavity and the output coupler. Up to a pulse repetition rate of 15 GHz we obtained average output power >1 W and pulse durations <4 ps. Furthermore we have been able to demonstrate the highest pulse repetition rate from any fundamentally modelocked semiconductor disk laser with 101.2 GHz at an average output power of 127 mW and a pulse duration of 570 fs.

OCIS codes: (140.3460) Lasers; (140.4050) Mode-locked lasers; (140.5960) Semiconductor lasers; (140.7090) Ultrafast lasers; (140.7270) Vertical emitting lasers.

References and links

1. P. W. Juodawlkis, J. C. Twichell, G. E. Betts, J. J. Hargreaves, R. D. Younger, J. L. Wasserman, F. J. O'Donnell, K. G. Ray, and R. C. Williamson, "Optically Sampled Analog-to-Digital Converters," IEEE Trans. Microw. Theory Tech. **49**(10), 1840–1853 (2001).
2. H. R. Telle, G. Steinmeyer, A. E. Dunlop, J. Stenger, D. H. Sutter, and U. Keller, "Carrier-envelope offset phase control: A novel concept for absolute optical frequency measurement and ultrashort pulse generation," Appl. Phys. B **69**(4), 327–332 (1999).
3. D. Hillerkuss, R. Schmogrow, T. Schellinger, M. Jordan, M. Winter, G. Huber, T. Vallaitis, R. Bonk, P. Kleinow, F. Frey, M. Roeger, S. Koenig, A. Ludwig, A. Marculescu, J. Li, M. Hoh, M. Dreschmann, J. Meyer, S. Ben Ezra, N. Narkiss, B. Nebendahl, F. Parmigiani, P. Petropoulos, B. Resan, A. Oehler, K. Weingarten, T. Ellermeyer, J. Lutz, M. Moeller, M. Huebner, J. Becker, C. Koos, W. Freude, and J. Leuthold, "26 Tbit s^{-1} line-rate super-channel transmission utilizing all-optical fast Fourier transform processing," Nat. Photonics **5**(6), 364–371 (2011).
4. U. Keller, K. J. Weingarten, F. X. Kärtner, D. Kopf, B. Braun, I. D. Jung, R. Fluck, C. Hönninger, N. Matuschek, and J. Aus der Au, "Semiconductor saturable absorber mirrors (SESAMs) for femtosecond to nanosecond pulse generation in solid-state lasers," IEEE J. Sel. Top. Quantum Electron. **2**(3), 435–453 (1996).
5. A. Schlatter, B. Rudin, S. C. Zeller, R. Paschotta, G. J. Spühler, L. Krainer, N. Haverkamp, H. R. Telle, and U. Keller, "Nearly quantum-noise-limited timing jitter from miniature Er:Yb:glass lasers," Opt. Lett. **30**(12), 1536–1538 (2005).
6. A. E. H. Oehler, M. C. Stumpf, S. Pekarek, T. Südmeyer, K. J. Weingarten, and U. Keller, "Picosecond diode-pumped 1.5 μm Er,Yb:glass lasers operating at 10–100 GHz repetition rate," Appl. Phys. B **99**(1-2), 53–62 (2010).

#204772 - $15.00 USD Received 14 Jan 2014; revised 18 Feb 2014; accepted 20 Feb 2014; published 7 Mar 2014

7. A. Klenner, M. Golling, and U. Keller, "A gigahertz multimode-diode-pumped Yb:KGW enables a strong frequency comb offset beat signal," Opt. Express **21**(8), 10351–10357 (2013).
8. D. C. Heinecke, A. Bartels, and S. A. Diddams, "Offset frequency dynamics and phase noise properties of a self-referenced 10 GHz Ti:sapphire frequency comb," Opt. Express **19**(19), 18440–18451 (2011).
9. C. Hönninger, R. Paschotta, F. Morier-Genoud, M. Moser, and U. Keller, "Q-switching stability limits of continuous-wave passive mode locking," J. Opt. Soc. Am. B **16**(1), 46–56 (1999).
10. M. Kuznetsov, F. Hakimi, R. Sprague, and A. Mooradian, "High-power (>0.5-W CW) diode-pumped vertical-external-cavity surface-emitting semiconductor lasers with circular TEM00 beams," IEEE Photon. Technol. Lett. **9**(8), 1063–1065 (1997).
11. U. Keller and A. C. Tropper, "Passively modelocked surface-emitting semiconductor lasers," Phys. Rep. **429**(2), 67–120 (2006).
12. M. Scheller, T. L. Wang, B. Kunert, W. Stolz, S. W. Koch, and J. V. Moloney, "Passively modelocked VECSEL emitting 682 fs pulses with 5.1W of average output power," Electron. Lett. **48**(10), 588–589 (2012).
13. K. G. Wilcox, A. C. Tropper, H. E. Beere, D. A. Ritchie, B. Kunert, B. Heinen, and W. Stolz, "4.35 kW peak power femtosecond pulse mode-locked VECSEL for supercontinuum generation," Opt. Express **21**(2), 1599–1605 (2013).
14. P. Klopp, U. Griebner, M. Zorn, and M. Weyers, "Pulse repetition rate up to 92 GHz or pulse duration shorter than 110 fs from a mode-locked semiconductor disk laser," Appl. Phys. Lett. **98**(7), 071103 (2011).
15. D. Lorenser, D. J. H. C. Maas, H. J. Unold, A.-R. Bellancourt, B. Rudin, E. Gini, D. Ebling, and U. Keller, "50-GHz passively mode-locked surface-emitting semiconductor laser with 100 mW average output power," IEEE J. Quantum Electron. **42**(8), 838–847 (2006).
16. K. G. Wilcox, A. H. Quarterman, V. Apostolopoulos, H. E. Beere, I. Farrer, D. A. Ritchie, and A. C. Tropper, "175 GHz, 400-fs-pulse harmonically mode-locked surface emitting semiconductor laser," Opt. Express **20**(7), 7040–7045 (2012).
17. K. G. Wilcox, A. H. Quarterman, H. E. Beere, D. A. Ritchie, and A. C. Tropper, "Repetition-frequency-tunable mode-locked surface emitting semiconductor laser between 2.78 and 7.87 GHz," Opt. Express **19**(23), 23453–23459 (2011).
18. O. D. Sieber, V. J. Wittwer, M. Mangold, M. Hoffmann, M. Golling, T. Südmeyer, and U. Keller, "Femtosecond VECSEL with tunable multi-gigahertz repetition rate," Opt. Express **19**(23), 23538–23543 (2011).
19. D. J. H. C. Maas, A.-R. Bellancourt, B. Rudin, M. Golling, H. J. Unold, T. Südmeyer, and U. Keller, "Vertical integration of ultrafast semiconductor lasers," Appl. Phys. B **88**(4), 493–497 (2007).
20. A.-R. Bellancourt, Y. Barbarin, D. J. H. C. Maas, M. Shafiei, M. Hoffmann, M. Golling, T. Südmeyer, and U. Keller, "Low Saturation Fluence Antiresonant Quantum Dot SESAMs for MIXSEL integration," Opt. Express **17**(12), 9704–9711 (2009).
21. B. Rudin, V. J. Wittwer, D. J. H. C. Maas, M. Hoffmann, O. D. Sieber, Y. Barbarin, M. Golling, T. Südmeyer, and U. Keller, "High-power MIXSEL: an integrated ultrafast semiconductor laser with 6.4 W average power," Opt. Express **18**(26), 27582–27588 (2010).
22. V. J. Wittwer, M. Mangold, M. Hoffmann, O. D. Sieber, M. Golling, T. Sudmeyer, and U. Keller, "High-power integrated ultrafast semiconductor disk laser: multi-Watt 10 GHz pulse generation," Electron. Lett. **48**(18), 1144–1145 (2012).
23. M. Mangold, V. J. Wittwer, C. A. Zaugg, S. M. Link, M. Golling, B. W. Tilma, and U. Keller, "Femtosecond pulses from a modelocked integrated external-cavity surface emitting laser (MIXSEL)," Opt. Express **21**(21), 24904–24911 (2013).
24. V. J. Wittwer, O. D. Sieber, M. Mangold, M. Hoffmann, C. J. Saraceno, M. Golling, B. W. Tilma, T. Südmeyer, and U. Keller, "First MIXSEL with a Quantum Well Saturable Absorber: Shorter Pulse Durations and Higher Repetition Rates," in *CLEO US 2012*(San Jose, 2012).
25. http://www.ulp.ethz.ch/research/FrequencyComb/GHzFrequencyCombs.
26. R. Häring, R. Paschotta, A. Aschwanden, E. Gini, F. Morier-Genoud, and U. Keller, "High–power passively mode–locked semiconductor lasers," IEEE J. Quantum Electron. **38**(9), 1268–1275 (2002).
27. D. J. H. C. Maas, B. Rudin, A.-R. Bellancourt, D. Iwaniuk, S. V. Marchese, T. Südmeyer, and U. Keller, "High precision optical characterization of semiconductor saturable absorber mirrors," Opt. Express **16**(10), 7571–7579 (2008).
28. A. Gosteva, M. Haiml, R. Paschotta, and U. Keller, "Noise-related resolution limit of dispersion measurements with white-light interferometers," J. Opt. Soc. Am. B **22**(9), 1868–1874 (2005).
29. O. D. Sieber, M. Hoffmann, V. J. Wittwer, M. Mangold, M. Golling, B. W. Tilma, T. Südmeyer, and U. Keller, "Experimentally verified pulse formation model for high-power femtosecond VECSELs," Appl. Phys. B **113**(1), 133–145 (2013).
30. M. Mangold, V. J. Wittwer, O. D. Sieber, M. Hoffmann, I. L. Krestnikov, D. A. Livshits, M. Golling, T. Südmeyer, and U. Keller, "VECSEL gain characterization," Opt. Express **20**(4), 4136–4148 (2012).
31. A.-R. Bellancourt, D. J. H. C. Maas, B. Rudin, M. Golling, T. Südmeyer, and U. Keller, "Modelocked Integrated External-Cavity Surface Emitting Laser (MIXSEL)," IET Optoelectronics **3**(2), 61–72 (2009).
32. M. Mangold, S. M. Link, A. Klenner, C. A. Zaugg, M. Golling, B. W. Tilma, and U. Keller, "Amplitude noise and timing jitter characterization of a high-power Mode-Locked Integrated External-Cavity Surface Emitting Laser," IEEE Photon. J. **6**(1), 1–9 (2014).

#204772 - $15.00 USD Received 14 Jan 2014; revised 18 Feb 2014; accepted 20 Feb 2014; published 7 Mar 2014

1. Introduction

High power ultrafast laser sources with high gigahertz pulse repetition rates can be used in a broad field of applications, such as high-resolution optical sampling [1], frequency metrology [2] and ultra high-speed and high-bandwidth communication systems [3]. Coherent optical communication requires low-noise sources such as diode-pumped solid-state lasers (DPSSLs) modelocked with a semiconductor saturable absorber mirror (SESAM [4]), which have quantum noise limited performance [5]. Thus fiber lasers have been replaced by SESAM modelocked Er:Yb:glass lasers [5, 6] for world record results in optical communication as described in Ref [3]. For frequency comb generation gigahertz DPSSLs have shown impressive performance recently [6–8], but they require more complex cavity setups and pumping schemes. In addition, they are not easily scalable to higher repetition rates as small gain cross-sections of the conventional ion-doped solid-state laser materials (typically in the order of $<10^{-19}$ cm^2) cause unwanted Q-switching instabilities at low intra-cavity pulse energy levels [9]. In contrast, optically pumped SESAM-modelocked semiconductor disk lasers (SDLs) or vertical-external-cavity surface-emitting lasers (VECSELs [10, 11]) can be fabricated using inexpensive wafer scale mass production at considerably lower costs, making this technology the most prominent candidate for widespread industrial applications. Those lasers are excellent candidates for such applications as they deliver femtosecond pulses with multi-watt average output power and excellent beam quality [12–14]. Furthermore, the large gain cross-sections of the semiconductor materials (in the order of 10^{-14} cm^2) and the simple cavity geometry enabled stable modelocking even at very high repetition rates up to 50 GHz in fundamental modelocking [15] and up to 175 GHz in harmonically modelocked operation [16]. In addition, continuous repetition rate tuning in femtosecond operation from 2.87 to 7.87 GHz [17] and from 6.5 to 11.3 GHz [18] has been demonstrated.

The modelocked integrated external-cavity surface emitting laser (MIXSEL [19]) combines the gain of VECSELs with the saturable absorber of a SESAM in a single integrated semiconductor layer stack.

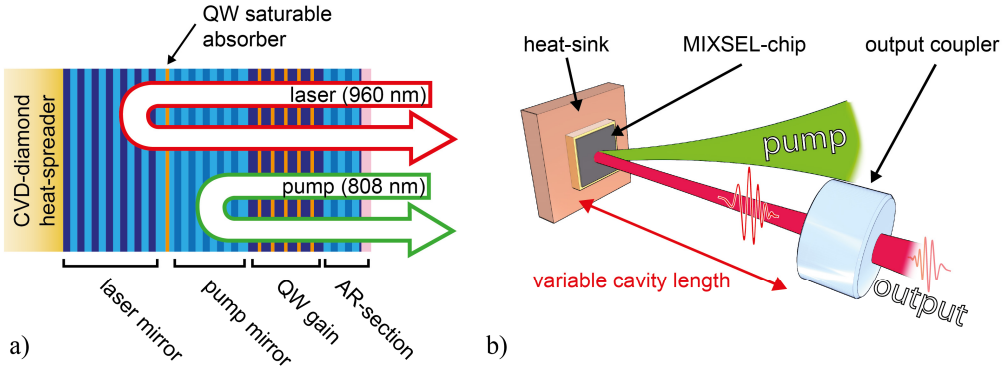

Fig. 1. a) MIXSEL-chip: The MIXSEL semiconductor layer stack is composed of a distributed Bragg reflector (DBR) for the lasing wavelength of around 960 nm and a DBR for the pump wavelength of 808 nm. In between the DBRs, a single low temperature grown InGaAs quantum well (QW) saturable absorber is placed. The active region is based on 10 InGaAs QWs embedded in GaAs for pump absorption. A hybrid semiconductor/fused silica anti-reflection section ensures low pump light reflection and low values of group-delay dispersion; b) Optically pumped MIXSEL: The MIXSEL-chip and a curved output coupler with typical transmission of <1% form a straight linear laser cavity. The flip-chip processed MIXSEL-chip is optically pumped by standard 808-nm diode laser arrays under an angle of ≈45°. The simple cavity design directly supports simple pulse repetition rate scaling of fundamental modelocking by mechanically adjusting the cavity length (i.e. the distance between the MIXSEL-chip and output coupler).

This concept enables high-power ultrafast semiconductor lasers with reduced complexity, packaging, and manufacturing cost. Self-starting and stable fundamental modelocking can be

#204772 - $15.00 USD Received 14 Jan 2014; revised 18 Feb 2014; accepted 20 Feb 2014; published 7 Mar 2014

achieved in a simple straight cavity, which is easily scalable to multi-100-GHz high repetition rates. The antiresonant MIXSEL design [20] allowed for multi-watt output power performance for the first time [21], even up to 10 GHz pulse repetition rates [22]. The antiresonant MIXSEL was based on an integrated single layer quantum dot (QD) saturable absorber with which we achieved an average output power of 6.4 W with a pulse duration of 28 ps at a pulse repetition rate of 2.5 GHz [21], which has been the highest average power from an ultrafast semiconductor laser demonstrated so far. Furthermore, repetition rate scaling up to 10 GHz resulted in 17.1-ps-pulses and 2.4 W average output power shortly after [22], but the long pulse duration and the slow recovery dynamics of the saturable absorber prevented a further increase in pulse repetition rate.

Recently we developed a fast saturable absorber that does not degrade during the MIXSEL integration. It is based on a low-temperature grown single InGaAs quantum well (QW) embedded into AlAs barrier layers [23]. AlAs barriers introduce oxygen defects that are more robust during the long annealing taking place to finish the MBE growth of the full MIXSEL structure. Operated close to the band edge this saturable absorber has low saturation fluence and fast recovery dynamics, which are key requirements for stable modelocking and shorter pulse durations. Integrated into a first MIXSEL structure we were able to increase the repetition rate to 20 GHz with slightly shorter pulse durations of 6.8 ps however with a low average output power of only 8 mW because the thermal management of the MIXSEL was not optimized yet [24]. Using the same saturable absorber with better thermal management we then demonstrated the first femtosecond MIXSEL with a pulse duration of 620 fs at 4.83 GHz repetition rate and 101 mW of average output power [23].

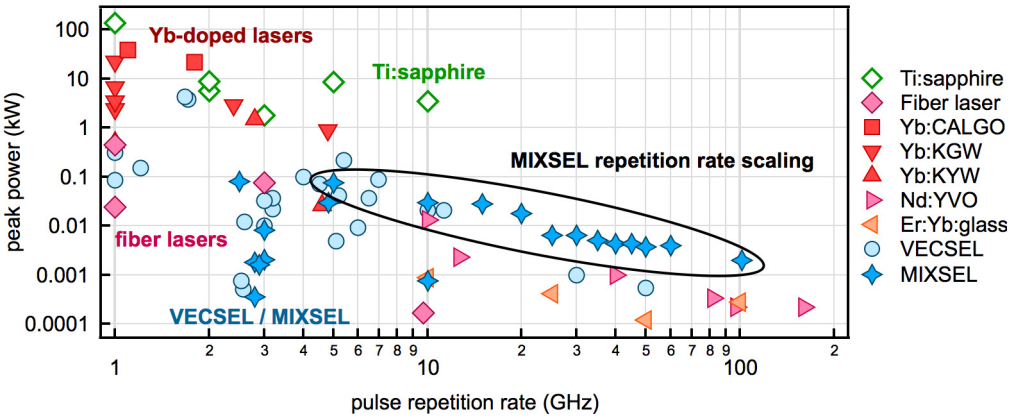

Fig. 2. Peak power of fundamentally modelocked lasers with gigahertz pulse repetition rates: The simple and inexpensive MIXSEL technology combines high-power with short pulse durations to achieve record-high average and peak power at >15 GHz pulse repetition rate [25].

Here, we demonstrate simple pulse repetition rate scaling from ≈5 GHz to 101.2 GHz, maintaining an excellent beam quality and good average output power for all individual measurements. This represents the largest scaling range of any gigahertz ultrafast laser technology based on the same laser setup. Up to 15 GHz, we achieved high average output power with >1 W and pulse durations of <4 ps (see Fig. 3). We substantially improved on the previous record 50-GHz repetition rate performance [15] with femtosecond MIXSEL operation at both 60 GHz and 101.2 GHz pulse repetition rates. At 101.2 GHz we also have generated the shortest pulses from a MIXSEL with a pulse duration of 570 fs. Furthermore to the best of our knowledge, in the pulse repetition rate range from 15 GHz to 101.2 GHz we obtained the highest average output power and highest peak power of any fundamentally modelocked laser (see Fig. 2).

#204772 - $15.00 USD Received 14 Jan 2014; revised 18 Feb 2014; accepted 20 Feb 2014; published 7 Mar 2014

2. MIXSEL concept and design

In a MIXSEL stable and self-starting fundamental passive modelocking can be achieved in a simple straight cavity, in which the semiconductor chip and a standard curved output coupler serve as cavity end mirrors (see Fig. 1(b)). By changing the distance between the cavity elements, the pulse repetition rate of the fundamentally modelocked MIXSEL can be varied easily over orders of magnitude without changing the laser setup fundamentally. The MIXSEL chip is optically pumped under an angle of 45° by a commercially available 808-nm diode array which is coupled into a multi-mode fiber with an M^2 of ≈75.

The MIXSEL structure was grown in a single run with a VEECO GEN III (Veeco instruments Inc., St. Paul, Minnesota) MBE machine in the FIRST cleanroom facility at ETH Zurich. The structure was grown in reverse epitaxial order with a single etch-stop layer placed between the undoped GaAs substrate and the structure for subsequent flip-chip bonding. After the epitaxy, the structure is bonded on a chemical-vapor-deposited diamond heat-spreader and the remaining substrate is removed [26].

Laser light at a wavelength of around 960 nm is reflected by an AlAs/GaAs distributed Bragg reflector (DBR), while the pump light is reflected by an AlAs/$Al_{0.2}Ga_{0.8}As$ DBR designed for the pump wavelength of 808 nm (see Fig. 1(a)). A single InGaAs QW absorber is placed between the two DBRs at the antinode of the standing wave pattern of the electric field intensity. For characterizing the saturable absorber, we have grown a SESAM with the same absorber properties as in the MIXSEL. Nonlinear reflectivity measurements were performed with 1.6-ps pulses at a wavelength of 960 nm for different SESAM temperatures with a setup described in [27]. In the temperature regime of 60-80°C at the absorber position, the modulation depth is found to be in the desired regime of 1-2% at saturation fluences of below 10 μJ/cm^2. Lower absorber temperatures lead to a modulation depth which is too low, whereas even higher absorber temperatures lead to linear absorber losses that stop the MIXSEL from reaching the laser threshold [23].

Table 1. Laser characteristics for pulse repetition rate scaling from 5 to 101.2 GHz

f_{rep} (GHz) / [l_{cav} (mm)]	τ_p (ps)	P_{out} (mW)	Δλ (nm) / [TBP]	P_{peak} (W) / [$P_{peak,\,ic}$ (kW)]	P_{pump} (W) / [w_{pump} (μm)]	output coupler ROC (mm) / [T_{OC} (%)]	F_{MIXSEL} (μJ/cm^2) / [w_{beam} (μm)]
5.1 / [29.4]	2.40	1050	0.80 / [1.98]	75.5 / [7.55]	17.2 / [144]	200 / [1]	30.6 / [148]
10 / [15.0]	3.86	1290	1.44 / [5.61]	29.4 / [4.20]	20.5 / [161]	500 / [0.7]	22.5 / [161]
15 / [10.0]	2.53	1130	1.32 / [3.40]	27.9 / [3.98]	22 / [144]	500 / [0.7]	16.0 / [146]
20 / [7.5]	1.72	692	2.48 / [4.29]	17.7 / [3.54]	25.1 / [144]	750 / [0.5]	9.7 / [151]
25 / [6.0]	2.26	410	1.78 / [4.07]	6.4 / [1.28]	16.9 / [126]	750 / [0.5]	5.1 / [143]
30 / [5.0]	1.86	405	1.40 / [2.63]	6.4 / [1.28]	14.8 / [144]	1000 / [0.5]	4.0 / [147]
35 / [4.3]	1.75	346	1.63 / [2.88]	5.0/ [0.99]	14.9 / [126]	1000 / [0.5]	3.2 / [141]
40 / [3.75]	1.51	301	1.74 / [2.66]	4.4/ [0.88]	15.0 / [126]	1000 / [0.5]	2.6 / [137]
45 / [3.33]	1.15	252	1.96 / [2.26]	4.3/ [0.85]	17.6 / [144]	1500 / [0.5]	1.7 / [147]
50 / [3.00]	1.68	350	1.55 / [2.63]	3.7 / [0.74]	14.9 / [144]	1500 / [0.5]	2.2 / [143]
60 / [2.50]	0.79	201	1.87 / [1.30]	4.0 / [0.80]	14.2 / [126]	1500 / [0.5]	1.1 / [137]
101.2 / [1.49]	0.57	127	2.62 / [1.50]	1.9 / [0.39]	20.1 / [126]	1500 / [0.5]	0.567 / [120]

f_{rep}: repetition rate, l_{cav}: cavity length, τ_p: pulse duration (sech^2-fit), P_{out}: average output power, Δλ: spectral bandwidth (FWHM), TBP: time-bandwidth product (in times of ideal value of 0.315 for sech^2-pulses), P_{peak}: peak power, $P_{peak,ic}$: intracavity peak power, P_{pump}: pump power, w_{pump}: beam waist of pump light, ROC: radius of curvature, T_{OC}: output coupler transmission, F_{MIXSEL}: fluence on MIXSEL, w_{beam}: calculated laser beam waist on MIXSEL.

The recovery dynamics of the absorber were measured with a time-resolved differential reflectivity measurement setup [28]. A double exponential fit to the measurement yields a fast

#204772 - $15.00 USD Received 14 Jan 2014; revised 18 Feb 2014; accepted 20 Feb 2014; published 7 Mar 2014

recovery time of τ_{fast} ≈380 fs and a slow recovery time of τ_{slow} ≈4.1 ps. The slow recovery time constant is therefore more than 40 times faster compared to the dynamics of the integrated saturable absorber of the previous QD-based MIXSEL [21, 22] and can support shorter pulse durations. The active region is based on ten compressively strained $In_{0.12}Ga_{0.88}As$ QWs embedded in GaAs. An anti-reflection (AR) section is grown on top of the active region. It is numerically optimized and consists of 3.5-pairs of $AlAs/Al_{0.2}Ga_{0.8}As$ and ends with a layer of fused silica that was deposited by plasma enhanced chemical vapor deposition after the flip-chip bonding process. The AR section reduces pump light reflection at the surface of the MIXSEL chip and provides a flat and slightly positive group delay dispersion (GDD) within ± 15 nm bandwidth centered around the design wavelength of 960 nm. A detailed description of the MIXSEL structure and a characterization of the integrated saturable absorber parameters are found in [23].

3. Experimental results

Table 1 and Fig. 3 summarize our results with regards to pulse repetition rate scaling. We changed the cavity length from 29.4 to 1.49 mm to tune the pulse repetition rate from 5.1 GHz to more than 100 GHz.

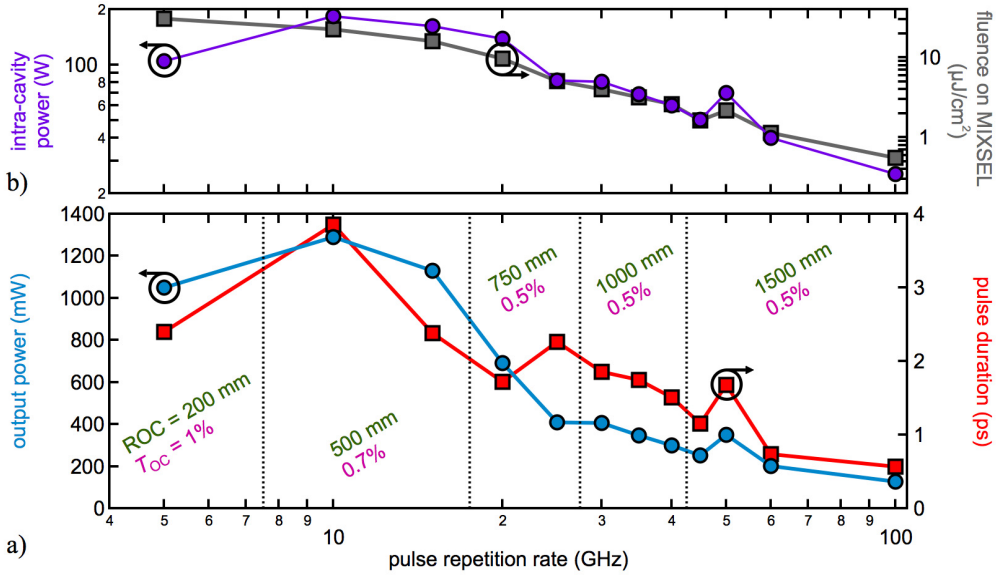

Fig. 3. Pulse repetition-rate scaling of high-power QW-absorber MIXSEL: a) Average output power (blue circles) and pulse duration (red squares) are given as a function of pulse repetition rates ranging from ≈5 GHz to 101.2 GHz. Output couplers with different radii of curvature (green) and transmissions (purple) ensure stable cavity configurations for the different cavity lengths. Watt-level operation was achieved up to 15 GHz and femtosecond pulse durations at 60 GHz and 101.2 GHz; b) Intracavity power (purple circles) and fluence on MIXSEL (gray squares) indicate a lower degree of absorber saturation with higher pulse repetition rates. This results in increased non-saturated absorber losses and reduced output power.

The transmission (T_{OC}) and the radius of curvature (ROC) of the output couplers had to be adapted to ensure stable laser and cavity configurations for a certain range of pulse repetition rates. For the 5.1 GHz pulse repetition rate, a T_{OC} = 1%, for 10 GHz and 15 GHz a T_{OC} = 0.7% was used, respectively. This supported watt-level average output power with a maximum of 1.29 W at 10 GHz pulse repetition rate. An even smaller output coupler transmission of T_{OC} = 0.5% had to be used for all higher pulse repetition rates to compensate for the weaker absorber saturation and therefore increased non-saturated losses of the MIXSEL.

#204772 - $15.00 USD Received 14 Jan 2014; revised 18 Feb 2014; accepted 20 Feb 2014; published 7 Mar 2014

By successively reducing the distance between the output coupler and the MIXSEL-chip from ≈30 mm to 3 mm, the pulse repetition rate was increased from ≈5 GHz to 50 GHz in steps of 5 GHz (see Fig. 3(a)). In this range from ≈5 GHz to 50 GHz, the pulse duration was measured to be below 4 ps for all measurements with a minimum of 1.15 ps at 45 GHz. By reducing the cavity length even more, the highest pulse repetition rate of any fundamentally modelocked SDL of 50 GHz [15] was surpassed, demonstrating a femtosecond MIXSEL with 60 GHz and 101.2 GHz repetition rate.

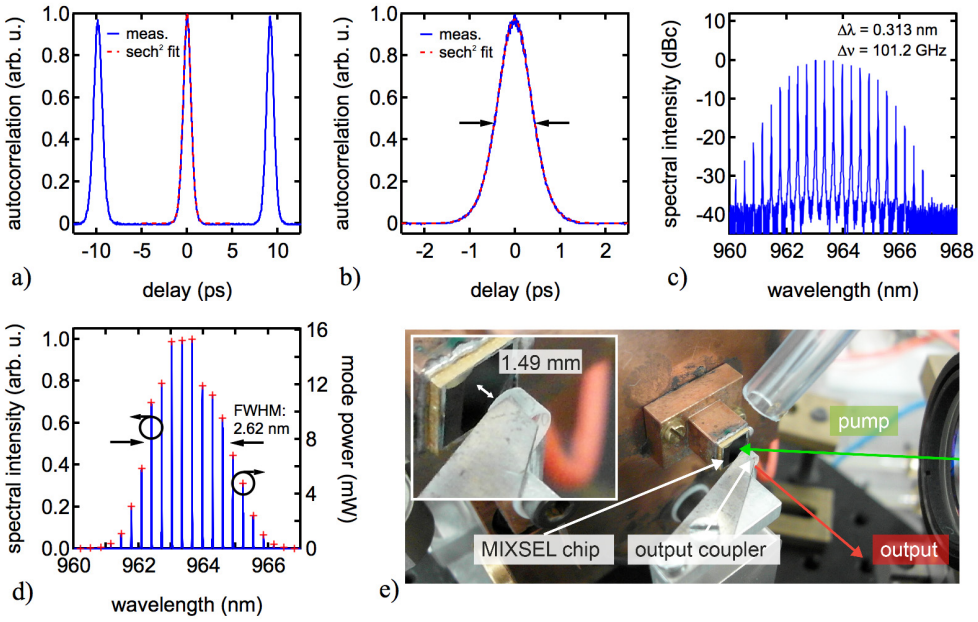

Fig. 4. MIXSEL with a pulse repetition rate of 101.2 GHz and 127 mW average output power: a) A long-delay autocorrelation with cross-correlation of preceding and subsequent pulses in distance of around 9.88 ps confirms single-pulse operation; b) A short delay autocorrelation with sech^2-fit precisely determines the pulse duration of 570 fs; c) The optical spectrum with a mode-spacing of 101.2 GHz (0.313 nm) is centered at 963.8 nm; d) The optical spectrum on a linear scale yields a bandwidth of 2.62 nm (FWHM), resulting in a time bandwidth product of 0.47 (1.5 times ideal sech^2) and 7.5 mW average power per mode (–30 dBc limit) and e) Picture shows the laboratory setup of the 1.49 mm long cavity.

At the highest pulse repetition rate of 101.2 GHz, 127 mW of average output power (see Fig. 4(e)) were measured. A long-delay autocorrelation (see Fig. 4(a)) including cross-correlations with preceding and subsequent pulses with a distance of the pulse repetition rate confirms stable fundamental passive modelocking at 101.2 GHz. A short-delay intensity autocorrelation trace with a fit to the autocorrelation of a sech^2-shaped pulse yields a pulse duration of 570 fs (see Fig. 4(b)). The optical spectrum with a resolution bandwidth of 10 pm is centered around 963.8 nm and the average longitudinal mode-spacing of 0.313 nm was used to precisely determine the pulse repetition rate (see Fig. 4(c)). The spectrum has a full width at half maximum (FWHM) of 2.62 nm, resulting in a time bandwidth product (TBP) of 0.47, which is 1.5 times the transform limit for sech^2-pulses (see Fig. 4(d)). The average power per longitudinal mode is 7.5 mW (–30 dBc limit) with a maximum of 15.3 mW in the most powerful mode. For the whole range of pulse repetition rates, excellent beam quality with $M^2 < 1.07 \pm 0.05$ was measured. The MIXSEL chip was kept at different temperatures between –4 °C and 10 °C to ensure optimum modelocking conditions for the varying cavity configurations. The pump power levels needed throughout the pulse repetition rate scaling were rather high and ranged between 14.2 W and 25.1 W.

#204772 - $15.00 USD Received 14 Jan 2014; revised 18 Feb 2014; accepted 20 Feb 2014; published 7 Mar 2014

For increasing pulse repetition rates the average output power and also the intracavity power drops (see Fig. 3(b)) Simulations revealed that the pulse formation in modelocked SDLs is based on a delicate balance between dynamic gain saturation, absorber saturation and intracavity GDD [29]. Reduced intracavity fluences (see Fig. 3(b) and Fig. 5) at higher repetition rates lead to higher saturable absorber losses (absorber saturation fluence $F_{\text{sat, absorber}}$ ≈7-10 μJ/cm^2). Those losses cannot be compensated by weaker saturation of the active QWs, which results only in a very little increase in gain (gain saturation fluence $F_{\text{sat, gain}}$ ≈50-70 μJ/cm^2 [30]). In contrast to ion-doped solid-state laser materials, increasing the small-signal gain by higher pump intensities is limited for a MIXSEL, since the ideal temperature gradient for spectral overlap between gain and absorber needs to be maintained inside the semiconductor structure. As discussed in more details in Ref [23] the MIXSEL structure with both the gain and the absorber is designed for a specific operation temperature taking into account the well defined red-shift of the bandgap with increasing temperature.

The pulse durations decrease for increasing pulse repetition rates. This is more complicated because multiple important parameters change. For example we have shown in similar VECSEL gain structures that the saturation fluence of the gain $F_{\text{sat, gain}}$ decreases with shorter pulse duration, e.g. 50 μJ/cm^2 for 1.4-ps pulses and 30 μJ/cm^2 for 130-fs probe pulses [30]. From 5 GHz to 100 GHz the pulse duration changes from ≈4 ps to 570 fs. In addition, the intracavity pulse fluence is significantly reduced at higher repetition rate, such that both the gain and the absorber are not strongly saturated anymore (see Fig. 5). Clearly we do not want to operate the MIXSEL with limited absorber saturation because this reduces the available output power and the overall efficiency. Work is in progress to optimize the design for specific operation parameters. This result however shows the great potential for the MIXSEL.

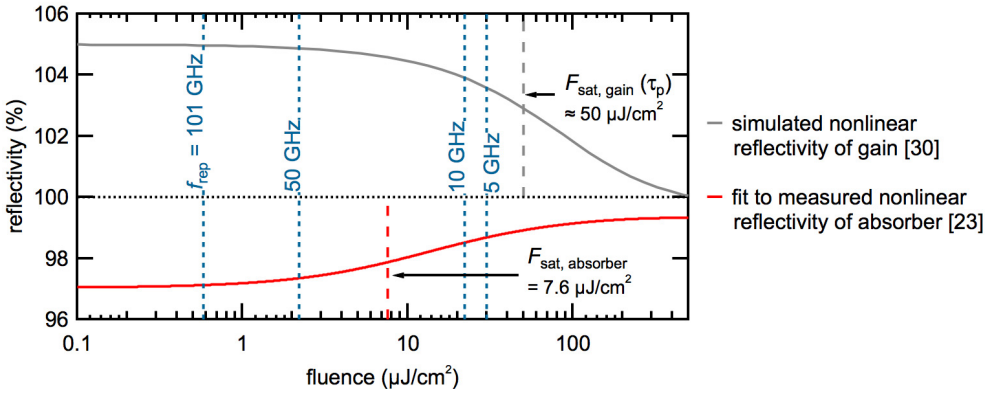

Fig. 5. Illustration of the nonlinear behavior of laser gain and saturable absorber: The simulated nonlinear reflectivity of the gain (grey) with an assumed small-signal gain of 5% (105% reflectivity) and a gain saturation fluence of $F_{\text{sat, gain}}$ ≈50 μJ/cm^2 [30] is compared to the fit of a measured nonlinear absorber reflectivity (red) with 2.3% modulation depth and a saturation fluence of $F_{\text{sat, absorber}}$ ≈7.6 μJ/cm^2 [23]. The intracavity fluences on the MIXSEL (blue) decrease significantly for higher pulse repetition rates. Therefore the low absorber saturation leads to high linear losses, which cannot be compensated by the weaker saturation of the gain.

The femtosecond pulse durations in principle could support even higher pulse repetition rates before the pulses start to temporally overlap inside the cavity. Reducing T_{OC} to increase the intracavity fluence and therefore the degree of absorber saturation comes at the expense of average output power. Further work is needed to obtain more average output power in this regime. At this point the current pumping geometry (i.e. pumping the MIXSEL-chip under an angle of 45°) sets a geometrical lower limit to the cavity length, before the pump beam is clipped by the output coupler. These geometrical boundaries can be overcome by pumping

#204772 - $15.00 USD Received 14 Jan 2014; revised 18 Feb 2014; accepted 20 Feb 2014; published 7 Mar 2014

the MIXSEL through a dichroic output coupler that is transparent for the 808-nm pump light, which should allow cavity geometries for significantly higher pulse repetition rates. Another possibility would be to pump the MIXSEL through the substrate, as has been proposed before [31].

4. Conclusion and outlook

We presented simple pulse repetition rate scaling of a high-power modelocked integrated external-cavity surface-emitting laser (MIXSEL) from ≈5 GHz to 50 GHz in steps of 5 GHz. From ≈5 GHz to 15 GHz we achieved watt-level operation in sub-4-ps pulses. We additionally demonstrated stable femtosecond operation at pulse repetition rates of 60 GHz and 101.2 GHz, achieving new world-record performance with the highest pulse repetition rate of any fundamentally modelocked SDL to date. In addition, operation at the highest pulse repetition rate resulted in the shortest pulses from a MIXSEL with a duration of 570 fs. To the best of our knowledge in this pulse repetition rate scaling study we achieved the highest average output power and highest peak power levels of any fundamentally modelocked laser between 15 GHz and 101.2 GHz and also demonstrated the largest gigahertz pulse repetition rate scaling range of any passively modelocked laser technology (see Fig. 2). For all measurements excellent beam quality with $M^2 < 1.07 \pm 0.05$ was obtained.

Key for this successful demonstration was the fast saturable absorber with a low saturation fluence and the broadband dispersion compensation. A fast low saturation fluence integrated saturable absorber was achieved with a single low-temperature grown InGaAs quantum well embedded in AlAs barrier layers. The dispersion was optimized with a broadband anti-reflection section with small group delay dispersion (GDD) centered at the lasing wavelength.

This novel MIXSEL is a unique high-power ultrafast laser source that can be used for applications in the field of optical clocking, optical communication and frequency metrology. Both the amplitude noise and the timing jitter of this laser is excellent and comparable to diode-pumped solid-state lasers [32]. The semiconductor gain material makes the MIXSEL technology not only more flexible in design and wavelength, but also avoids Q-switching instabilities at very high pulse repetition rates and low intracavity pulse energy levels. Further optimization of the structure and absorber should result in a better optical-to-optical efficiency and together with mode-size power scaling femtosecond operation at watt-level average output power is expected in a broad range of gigahertz pulse repetition rates.

Acknowledgments

The authors acknowledge support of the technology and cleanroom facility FIRST of ETH Zurich for advanced micro- and nanotechnology. This work was financed by the Swiss Confederation Program Nano-Tera.ch, which was scientifically evaluated by the Swiss National Science Foundation (SNSF).